Biology of Reproduction, 2017, 97(4), 612–621
doi:10.1093/biolre/iox122
Additions and Corrections
Advance Access Publication Date: 4 October 2017

Additions and Corrections

The developmental origin and compartmentalization of glutathione-s-transferase omega 2 isoforms in the perinuclear theca of eutherian spermatozoa†

Lauren E Hamilton[1], Genevieve Acteau[1], Wei Xu[1], Peter Sutovsky[2,3] and Richard Oko[1,*]

[1]Department of Biomedical and Molecular Sciences, Queen's University, Kingston, Ontario, Canada; [2]Division of Animal Sciences, College of Food, Agriculture and Natural Resources, School of Medicine, University of Missouri, Columbia, Missouri, USA and [3]Department of Obstetrics, Gynecology and Women's Health, School of Medicine, University of Missouri, Columbia, Missouri, USA

*__Correspondence:__ Department of Biomedical and Molecular Sciences, Botterell Hall, Rm 849, Queen's University, Kingston, Ontario K7L 3N6, Canada. Tel: 613-533-2858; Fax: 613-533-2022; E-mail: ro3@queensu.ca

†__Grant Support:__ This study was supported by the Natural Sciences and Engineering Research Council of Canada (RGPIN/192093) (RO), Agriculture and Food Research Initiative Competitive grant no. 2015-67015-23231 from the USDA National Institute of Food and Agriculture (PS), as well as by seed funding from the Food for the 21st Century Program of the University of Missouri (PS).
__Conference Presentation:__ Presented as part of the 2016 Gordon Research Conference on Mammalian Reproduction, 21–26 August 2016, Waterville Valley, New Hampshire, United States of America.

Received 19 May 2017; Revised 16 August 2017; Accepted 29 September 2017

Abstract

The perinuclear theca (PT) is a condensed, nonionic detergent resistant cytosolic protein layer encapsulating the sperm head nucleus. It can be divided into two regions: the subacrosomal layer, whose proteins are involved in acrosomal assembly during spermiogenesis, and the postacrosomal sheath (PAS), whose proteins are implicated in sperm–oocyte interactions during fertilization. In continuation of our proteomic analysis of the PT, we have isolated two prominent PT-derived proteins of 28 and 31 kDa from demembranated bovine sperm head fractions. These proteins were identified by mass spectrometry as isoforms of glutathione-s-transferase omega 2 (GSTO2). Immunoblots probed with anti-GSTO2 antibodies confirmed the presence of the GSTO2 isoforms in these fractions while fluorescent immunocytochemistry localized the isoforms to the PAS region of the bull, boar, and murid PT. In addition to the PAS labeling of GSTO2, the performatorium of murid spermatozoa was also labeled. Immunohistochemistry of rat testes revealed that GSTO2 was expressed in the third phase of spermatogenesis (i.e., spermiogenesis) and assembled in the PAS and perforatorial regions of late elongating spermatids. Fluorescent immunocytochemistry performed on murine testis cells co-localized GSTO2 and tubulin on the transient microtubular-manchette of elongating spermatids. These findings imply that GSTO2 is transported and deposited in the PAS region by the manchette, conforming to the pattern of assembly found with other PAS proteins. The late assembly of GSTO2 and its localization in the PAS suggests a role in regulating the oxidative and reductive state of covalently linked spermatid/sperm proteins, especially during the disassembly of the sperm accessory structures after fertilization.

Summary Sentence

GSTO2 isoforms are prominent constituents of the perinuclear theca and are deposited in this sperm head region by the microtubular-manchette late in spermiogenesis.

Key words: GSTO, sperm, perinuclear theca, postacrosomal sheath, spermatogenesis, spermiogenesis, microtubular manchette, proteomics, murids, ruminants, swine.

Introduction

The perinuclear theca (PT) is a dense cytosolic protein layer that acts as a key cytoskeletal component of the sperm head [1]. It lies under the acrosome and surrounds the entire condensed nucleus of mature spermatozoa, except for the tail implantation fossa [1–7]. The PT can be compositionally and functionally divided into two regions: the subacrosomal layer (SAL, including the outer periacrosomal layer in the equatorial segment region) and the postacrosomal sheath (PAS) [1]. The SAL proteins are involved in acrosomic vesicle transport and attachment to the spermatid nucleus as well as the expansion of the acrosomal cap during spermiogenesis [1]. Conversely, PAS proteins are implicated in sperm–oocyte interactions during fertilization, such as oocyte activation and pronuclear formation [1].

The current paradigm of PT development states that it is formed in two stages. In the early steps of spermiogenesis, the SAL emerges during acrosomal formation. In contrast, the PAS assembles in the second half of spermiogenesis, commensurate with the caudal descent of the microtubular manchette, which initially forms a girdle around the spermatid nucleus just below the acrosome [1, 7, 8]. The distal region of the manchette reaches far into the spermatid cytoplasm surrounding the nascent sperm tail (the cytoplasmic lobe). A cytoplasmic channel surrounding the nucleus forms from the positioning of the manchette and is filled with microtubules that connect the spermatid head with the cytoplasmic lobe. This positioning suggested that the manchette could be an important shuttle that delivers proteins from the cytoplasmic lobe to the forming caudal section of the future sperm head by a process termed intramanchette transport (IMT) [9–13]. The discovery that molecular motor proteins, kinesins and dyneins, are associated with the manchette lends support to this hypothesis [13–16]. Further support for IMT transport came from colocalization studies showing that major PAS proteins (i.e., postacrosomal sheath WW-domain binding protein [WBP2NL/PAWP] and the four core somatic histones) are distributed on the microtubules of the manchette before their deposition and encapsulation around the caudal half of the spermatid nucleus in the wake of manchette descent [17, 18]. In bovine spermiogenesis, the descent of the manchette and assembly of the PAS occurs between steps 11 and 12 [8, 9], while in the mouse, it occurs between steps 13 and 14 [18].

In this study, we sequence identified and characterized two more PAS members whose pattern of assembly during spermiogenesis supports IMT and is in agreement with previously described developmental origins of PAS proteins [17, 18]. Our data support the hypothesis of the existence of two compositionally and functionally distinct regions of the PT with subacrosomal layer perinuclear theca (SAL-PT) proteins acting during acrosome assembly [19–21] and postacrosomal sheath perinuclear theca (PAS-PT) proteins functioning in sperm–oocyte interactions [22–24]. Additionally, our findings highlight the newly identified PAS-anchored glutathione-s-transferase omega 2 (GSTO2) isoforms as potential contributors to sperm–egg interactions, which are vital for zygotic development after fertilization. Being members of the Omega class of glutathione-s-transferase (GST) enzymes, we hypothesize that they function in the breakdown of disulfide-bonded proteins/structures, which surround or are within the sperm nucleus, soon after sperm–egg fusion. This would insure the timely degradation of sperm cytoskeletal structures and the decondensation of the sperm nucleus, a prerequisite for the formation of a paternal pronucleus.

Materials and methods

Animals

For all mouse studies, mature male retired CD1 breeders were purchased from Charles River Laboratories (Charles River, St-Constant, QC, Canada). All procedures were performed in accordance with the Animal Utilization Protocols approved by the Queen's Animal Care Committee and complied with the Guidelines of Canada Council on Animal Care. Bovine samples were collected from bull testes and epididymides donated by Hilts Butcher Shop Ltd Norwood, ON.

Preparation of bovine spermatozoa

Bovine spermatozoa were collected into phosphate-buffered saline (PBS) by creating incisions along the epididymis and allowing the spermatozoa to swim out. The sperm solution was subsequently filtered through fine mesh netting to remove any residual tissue. The solution was centrifuged at 1000 × *g* for 5 min and the supernatant was discarded. The spermatozoa were resuspended in PBS, and phenyl methylsulphonyl fluoride and protease inhibitor cocktail suspensions were added to the solution. The solution was sonicated on ice at 40 Hz using a Vibracell sonicator (Sonics & Materials Inc., Danbury, CT) at 10-s bursts with 1-min interval (usually three times), until >99% of all sperm heads and tails were dissociated. Sonication also disrupted the plasmalemma and the acrosome, releasing its contents. Spermatozoa were then centrifuged at 1000 × *g* and pellet resuspended in an 80% sucrose solution and ultracentrifuged at 50 000 RPM for 2 h in a 70Ti angle rotor (Beckman, Mississauga, Canada; Figure 1A). Ultracentrifugation pellets the heads, which are denser than the 80% sucrose, on the centrifugal side of the tube and the tails on the inner wall of the tube [20]. The sperm heads and tails were then removed and placed in separate tubes and used directly or frozen for later use.

Preparation of mouse spermatozoa

Caput and cauda epididymides were removed from mature male retired CD1 breeders and were placed in 2 ml of tris buffered saline (TBS) (pH 7.5–8) solution. Cuts were then made along the epididymis to allow the spermatozoa to swim out. The sperm solution was placed in Eppendorf tubes and washed through centrifugation twice at 1000 × *g* for 5 min. Spermatozoa were either used immediately or stored at –80°C for future use. Testis extracts were obtained by removing the tunica albuginea from the testis of male retired CD1 breeders in 2 ml of 200 mM PBS. Cuts were then made in the seminiferous tubules to allow the spermatids to diffuse into the solution.

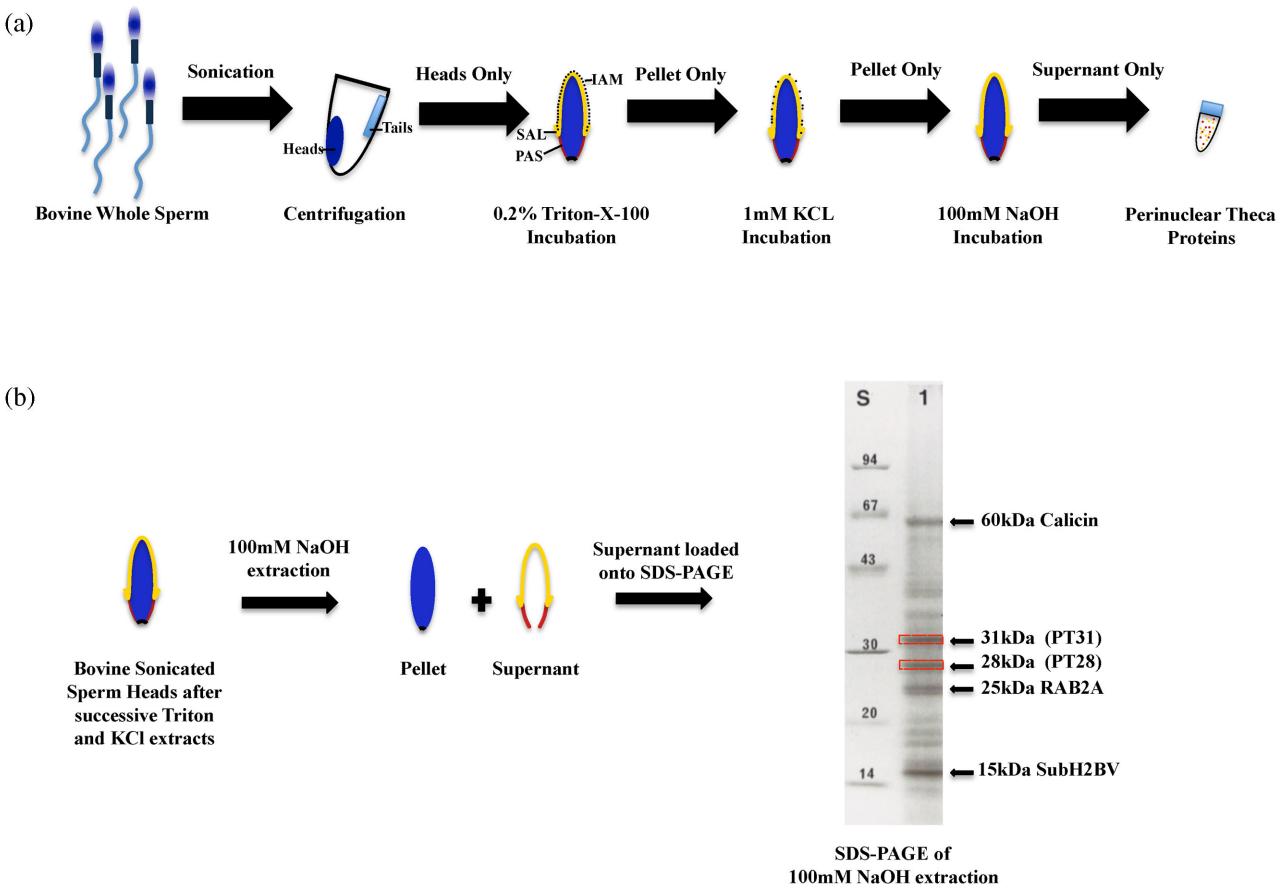

Figure 1. (A) Steps involved with the isolation of bovine sonicated sperm heads and the successive extractions (Triton, KCL, and NaOH) performed to isolate the PT proteins. (B) The SDS-PAGE of the 100 mM NaOH extraction of sonicated bovine sperm heads. The two perinuclear bands (PT28 and PT31) that were excised and sequenced are highlighted with red boxes. Other prominent bands displayed have previously been identified as PT proteins. [A color version of this figure is available in the online version.]

Protein identification

Sonicated bovine sperm heads were incubated in a sequential series of detergents to extract protein fractions based on their chemical bonding properties. The series of detergents were utilized in the following order: 0.2% Triton-X-100 (1 h), 1M KCl (1 h), and 100 mM NaOH (overnight) with agitation at 4°C (Figure 1A and B). Following the incubations, the solution was subjected to centrifugation at 2500 × *g* for 10 min at 4°C and the resulting supernatants were recovered. The head pellets were washed twice with PBS before the next extraction step. The first extraction step removes solubilized proteins from the inner acrosomal membrane, and the second step extracts ionically bound proteins from the PT. Of interest in this study is the last extraction, which releases covalently bound or structurally trapped PT proteins. The detergent fractions were separated by sodium dodecyl sulfate-polyacrylamide gel (SDS-PAGE) electrophoresis and the gel was subsequently stained with Coomassie Brilliant Blue 250 (Sigma, St. Louis, MO) to identify the predominant protein bands of the PT. The 28 and 31 kDa bands were cut out of the gel and digested using the Micromass MassPREP Robotic Protein Handling System (PerkinElmer). The trypsin-digested samples were analyzed by the SCIEX Voyager DE Pro matrix-assisted laser-desorption (MALDI) mass spectrometer at the Protein Function Discovery Facility of Queen's University, Ontario, Canada. Data from peptide mass fingerprinting were acquired over the mass range of m/z 800–3400. The MS data were analyzed using Applied Biosystems Data Explorer version 5.1 and entered into the Genebio Aldente search engine for comparison against the Swiss-Prot database.

Protein extractions

Bovine whole sperm and sonicated spermatozoa were treated in serial extractions to investigate GSTO2 extractability, and the series of detergents used were as follows: 1% NP-40 (2 h) and 1% sodium dodecyl sulfate (SDS) (2 h). Following the incubations, the solution was subjected to centrifugation at 2500 × *g* for 10 min and the resulting supernatants were recovered. The resulting pellets were washed twice with PBS before the next extraction and/or before being digested/solubilized in reducing sample buffer.

Antibodies

Four primary antibodies were used in the presented experiments. A polycolonal goat anti-GSTO2 (Y-12; Santa Cruz) was used at a concentration of 1:500 for western blot analysis, and at a concentration of 1:30 for fluorescent immunocytochemistry. An affinity purified rabbit polyclonal anti-GSTO2 (SAB1401977; Sigma) was used at a concentration of 1:200 for western blot analysis. An affinity purified rabbit polyclonal anti-GSTO2 (HPA048141; Sigma) was used at a concentration of 1:5 for enzymatic immunohistochemistry. Lastly,

a mouse monoclonal anti-α-tubulin (T6074; Sigma) was used at a concentration of 1:50 for fluorescent immunocytochemistry. For western blot analysis, the secondary antibodies used were donkey anti-goat IgG-HRP (sc-2033; Santa Cruz) at a concentration of 1:10 000 and goat anti-rabbit IgG HRP (PI-1000; Vector Laboratories) at a concentration of 1:10 000. For fluorescent immunocytochemistry, the secondary antibodies used were donkey anti-goat CFL 555 (sc-326625; Santa Cruz) at a concentration of 1:100, donkey anti-rabbit CFL488 (sc-362261; Santa Cruz) at a concentration of 1:100, and donkey anti-mouse antibody (sc-362288; Santa Cruz) at a concentration of 1:100. The secondary antibody used for immunohistochemistry was biotinylated goat-anti-rabbit IgG (PK-4001; Vector Laboratories) at a concentration of 1:200. Blocking peptide (Y-12P; Santa Cruz) was used at a 2:1 peptide-antibody ratio for all applicable experiments.

Gel electrophoresis and immunoblotting

Whole bovine, murine, and rat spermatozoa, and sperm head fractions (supernatants and pellets) were dissolved in reducing sample buffer (200mM Tris pH 6.8, 4% SDS, 0.1% bromophenol blue, 40% glycerol, and 5% β-mercaptoethanol) and run on SDS-PAGE along with a Blueye prestained protein marker (GeneDirex) according to Laemmli [25]. Proteins separated by SDS-PAGE were transferred to polyvinylidene fluoride (PVDF) membranes (Biorad, Hercules, CA), according to the western transfer technique proposed by Towbin et al. [26]. PVDF membranes were blocked with 10% skim milk diluted in PBS-0.05%T20 (PBS, 0.05% Tween20 pH 7.4) at room temperature for 30 min. PVDF membranes were incubated in primary antibody in 2% skim milk diluted with PBS-0.05%T20 overnight at 4°C. For blocking experiments, the primary antibody was preincubated with its corresponding blocking peptide for 2 h at room temperature with continuous agitation before primary antibody incubation with the membrane. Blots were washed with PBS-0.05%T20 six times for 5 min each on a shaker for continuous agitation. Blots were subsequently incubated in secondary antibody conjugated with HRP for 3 h at room temperature. They were washed again with PBS-0.05%T20 six times for 5 min each on a shaker with continuous agitation. Lastly, they were incubated in BioRad Clarity Western ECL substrate (Biorad, Hercules, CA) for 5 min and exposed to X-Ray film (Eastman Kodak Company, Rochester, NY) for developing.

Fluorescent immunocytochemistry

Spermatozoa were suspended in PBS and placed into a 300 μl droplet of KMT Buffer (10 mM KCl, l mM MgCl2, and 10 mM Tris-HCl pH 7) on poly-L-lysine coated coverslips and left to adhere for 20 min at room temperature. The KMT buffer solution was removed and spermatozoa were fixed to the coverslip with 300 μl of 4% paraformaldehyde for 40 min at room temperature. The 4% paraformaldehyde was discarded and the spermatozoa were incubated in PBS, with 0.01% Triton-X-100 (PBS-0.01%T) for 40 min. Spermatozoa were blocked with 3% BSA (bovine serum albumin), diluted in PBS, for 25 min at room temperature and then incubated in primary antibody made in 1% BSA–PBS overnight at 4°C. Coverslips were rinsed five times with 1% BSA–PBS and incubated in secondary antibody solution containing DAPI (4′,6-Diamidino-2-Phenylindole, Dihydrochloride; conc. 1:100) for 40 min at room temperature and protected from light. Coverslips were rinsed again five times with PBS and placed cells down on glass slides with a drop of VectaShield Mounting Media (Vector Laboratories, Inc, Burlingame, CA). For blocking experiments, the primary antibody was preincubated with its corresponding blocking peptide for 2 h at room temperature with continuous agitation before primary antibody incubation. Slides were sealed with clear nail polish and stored in the dark at 4°C until imaged. Images were captured using a Quorum Wave Effects Spinning Disc Confocal machine at the Queen's University Biomedical Imaging Center as well as a Nikon Eclipse 800 microscope with CoolSnap CCD camera at the University of Missouri–Columbia and all images were analyzed using MetaMorph Imaging Software.

Enzymatic immunohistochemistry

Rat testicular sections were cut into 5 μm sections from testes that had been perfused with Bouin fixative and embedded in paraffin. The sections were deparaffinized in xylene and hydrated through a graded series of ethanol solutions. During the hydration process, the sections were treated to remove endogenous peroxidase activity, to neutralize picric acid, and to block free aldehyde groups [27]. After hydration, sections were exposed to antigen retrieval by microwaving in a 0.01 M sodium citrate solution (pH 6) [27]. Nonspecific binding was blocked with avidin and biotin blocking serum (Vector Laboratories, Inc., Burlingame, CA). Primary antibody was incubated overnight at 4°C in a high-humidity chamber. Normal rabbit serum served as a negative control. Sections were washed four times for 5 min in Tris saline buffer containing 0.1% Tween-20 pH 7.4 (TBS-0.1%T) and incubated with secondary antibody for 30 min. Sections were washed four times for 5 min each in TBS-0.1%T and then incubated with an avidin–biotin complex kit (PK-4001; Vector Laboratories, Inc., Burlingame, CA) according to the Vector Lab protocol. After washing in TBS-0.1%T, peroxidase reactivity was excited by incubating the sections with DAKO Liquid DAB-Substrate Chromogen System (Dako North America, Inc., Carpinteria, CA) for 10 min in accordance with the instructions provided by Dako. The sections were then washed with distilled water and counterstained with 0.1% filtered methylene blue, followed by immersion in tap water. The sections were dehydrated, cleared in xylene, and mounted to coverslips using Permount (FisherScientific, Fair Lawn, NJ). Sections were visualized through light microscopy.

Results

The presence of glutathione-s-transferase omega 2 in the perinuclear theca of mature mammalian spermatozoa

Alkaline extracts of sonicated bovine sperm heads were analyzed by SDS-PAGE. Commassie Brilliant Blue 250 staining revealed two prominent protein bands of 28 and 31 kDa that were previously unidentified (Figure 1B). These presumably perinuclear bands, tentatively designated PT28 and PT31, were extracted and analyzed for sequence identity by mass spectrometry (Figure 2A and B). Each was found to contain, as a repeatable major match and significant database hit, a different isoform of GSTO2 with deduced molecular masses of 30.2 and 37.6 kDa, respectively (Figure 3). The sequence coverage between PT31 and the higher mass isoform of GSTO2 was 42% and between PT28 and the lower mass isoform was 36%. As far as we are aware, this is the first report of a 37 kDa isoform of GSTO2 residing in a tissue, with an extended amino-terminal end not previously recorded for GSTO2 in GeneBank (Figure 3).

Immunoblotting on whole bovine spermatozoa, as well as sonicated and isolated sperm heads (SspH) and tails showed that GSTO2 resided in the heads of bovine spermatozoa (Figure 4A). Further immunoblotting on a successive series of detergent extractions of whole

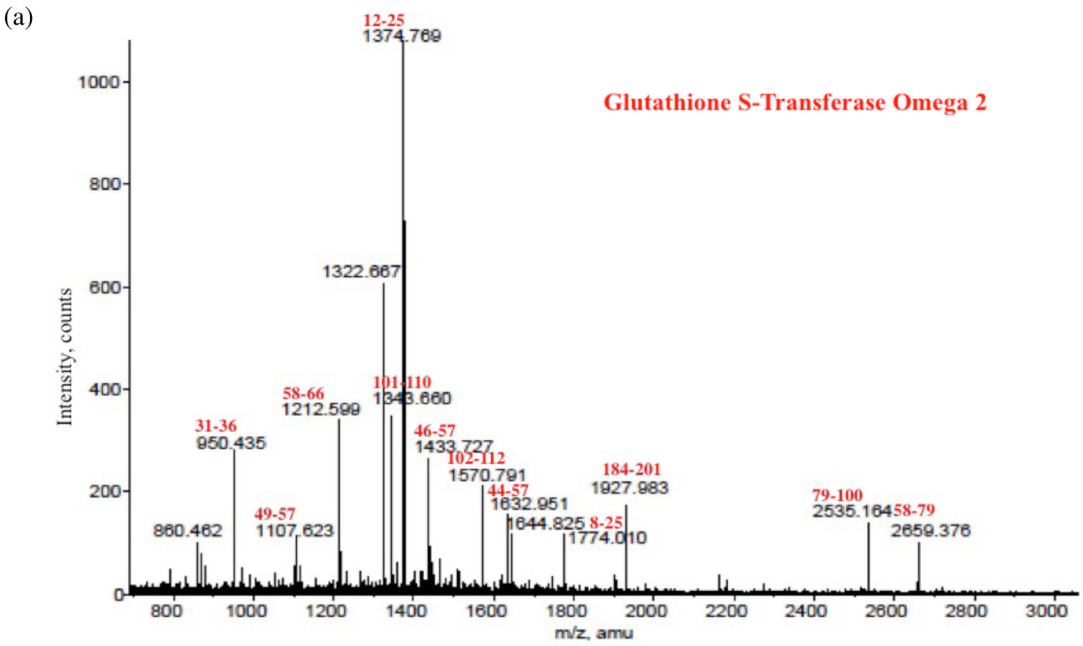

MALDI spectrum of the in-gel tryptic digest of PT28

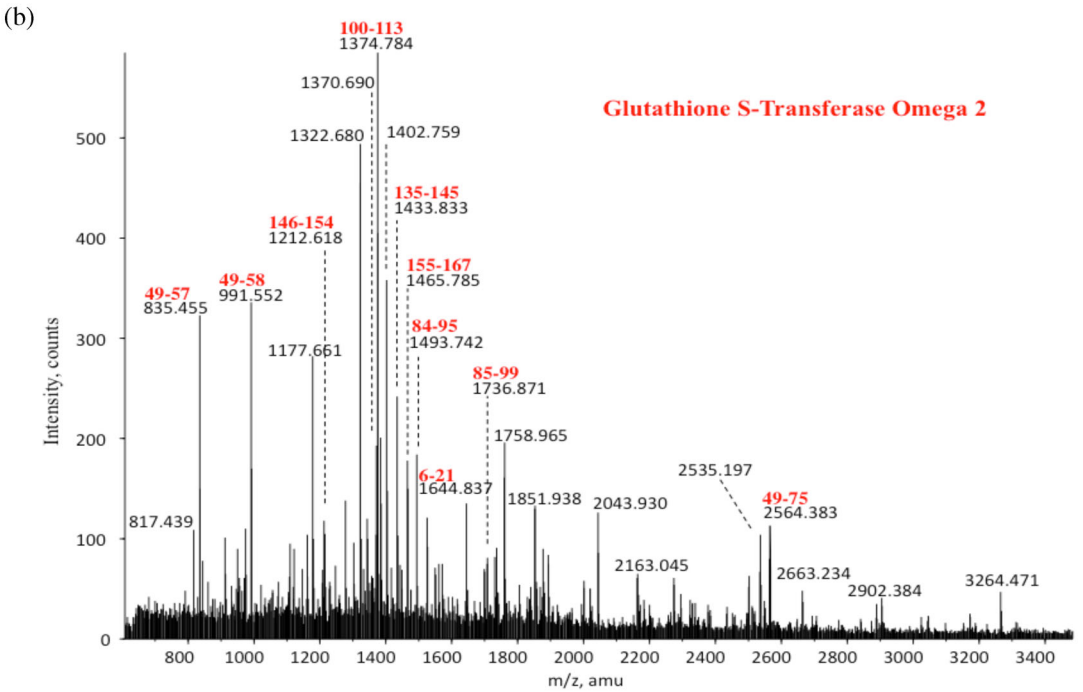

MALDI spectrum of the in-gel tryptic digest of PT31

Figure 2. The MALDI MS mass spectrometry results for PT28 (A) and PT31 (B). The red numbers above the peaks signify the correlating peptide sequence within the proteins amino acid sequences shown in Figure 3. [A color version of this figure is available in the online version.]

Genebank GSTO2 Sequence

```
  1 MTDDATRTLG KGSIPPGPVP EGVIRLYSMR FCPYAHRTRL VLRAKGIRHE
 51 VININLRNKP EWYFTKHPFG QIPVLENSKC QLIYESVIAC EYLDDAYPGR
101 KLYPYDPYER ARQKMLLELF YKVPHLTKEC LVALRCGRDC GDLKLALRQE
151 FCNLEEILGY QNTVFFGGDC ISMIDYLFWP WFERLEVYGI ADCVNHTPAL
201 RLWIAAMKQD PTVCSLLTDK NTFLGFLNLY FQNNPGAFDY GLSC
```

PT28 Sequence

```
  1 MTDDATRTLG KGSIPPGPVP EGVIRLYSMR FCPYAHRTRL VLRAKGIRHE
 51 VININLRNKP EWYFTKHPFG QIPVLENSKC QLIYESVIAC EYLDDAYPGR
101 KLYPYDPYER ARQKMLLELF YKVPHLTKEC LVALRCGRDC GDLKLALRQE
151 FCNLEEILGY QNTVFFGGDC ISMIDYLFWP WFERLEVYGI ADCVNHTPAL
201 RLWIAAMKQD PTVCSLLTDK NTFLGFLNLY FQNNPGAFDY GLSC
```

PT31 Sequence

```
  1 MPTLRADSSL LPSACPTQQA RVRCGRTSVG SAVLDHFPTT PTRPCCSKVA
 51 FGASGARRNV AVLGPCAGGS KPHGKDCERW SLRRRRESMT DDATRTLGKG
101 SIPPGPVPEG VIRLYSMRFC PYAHRTRLVL RAKGIRHEVI NINLRNKPEW
151 YFTKHPFGQI PVLENSKCQL IYESVIACEY LDDAYPGRKL YPYDPYERAR
201 QKMLLELFYK VPHLTKECLV ALRCGRDCGD LKLALRQEFC NLEEILGYQN
251 TVFFGGDCIS MIDYLFWPWF ERLEVYGIAD CVNHTPALRL WIAAMKQDPT
301 VCSLLTDKNT FLGFLNLYFQ NNPGAFDYGL SC
```

Figure 3. The protein sequences of PT28 and PT31 in comparison to the sequence of GSTO2 found in the GeneBank for *Bos taurus*. The amino acids highlighted in red are peaks identified through mass spectrometry. The sequence underlined in blue is the newly identified amino-terminal extension of GSTO2 not previously recorded. [A color version of this figure is available in the online version.]

bull spermatozoa were performed to establish the extractability of GSTO2 (Figure 4B). The GSTO2 protein is relatively unextractable in NP-40 (nonionic detergent) and not completely extractable in SDS (ionic detergent) with a sizeable portion remaining in the pellet after successive extractions in these detergents. Similar results were seen in a series of detergent extractions on whole rat spermatozoa. The exception was that the higher molecular mass isoform was almost completely extractable by SDS (Figure 4C). These results agree with the characterization of GSTO2 solubility in other tissues and its high cysteine content [28]. The relative resistance to extraction in nonionic detergents along with the retention of the two isoforms in SspH (see Figure 1B), but not the isolated tails, indicated that GSTO2 most likely resided in the PT of the sperm head. To verify the specificity of the anti-GSTO2 antibody, the antibody was preincubated with the GSTO2 peptide it was raised against before immunoblotting (Figure 4D).

Investigations into the localization of GSTO2 were performed on bovine, porcine, murine, and rat spermatozoa by fluorescent immunocytochemistry and revealed its presence in the PAS region of the PT (Figure 5A–D), suggesting an evolutionary conservation of GSTO2 as a constituent of the PT in eutherians. The GSTO2 isoforms were also found to reside in the perforatorium region of both the mouse and rat (Figure 5C and D). The immunofluoresecent labeling of GSTO2 was absent when the antibody was preincubated with a blocking peptide corresponding to the sequence it was raised against, thus confirming the antibody's specificity (Figure 5E–H)

The developmental origin of glutathione-s-transferase omega 2 during spermiogenesis

To investigate if GSTO2 follows a similar developmental localization pattern as other PAS proteins, we performed immuno-peroxidase histochemistry on rat testis sections (Figure 6). Immunoreactivity of the postacrosomal and perforatorial regions of the PT of spermatids was not observed until after step 15 of the 19 steps of rat spermiogenesis. In step 16 spermatids, just after the microtubular manchette's descent, the caudal region of elongating spermatid heads was strongly reactive, indicative of PAS staining, while the extreme-apical region of the heads was moderately reactive, indicative of perforatorial staining (Figure 6A). By step 18, the immunoreactivity of both head regions of the PT was greatly increased (Figure 6B). Therefore, the developmental pattern of GSTO2 is similar to the pattern shown with other PAS proteins such as WBP2NL/PAWP and the four core somatic core histones [17, 18]. Since these two proteins were shown to be transported by the microtubular manchette to their site of assembly in the PAS, we speculated that GSTO2 would use this route as well.

We confirmed the association of GSTO2 and tubulin by immunofluorescent colocalization on the manchette (Figure 7). These findings suggest that GSTO2 initially associates with the microtubules of the manchette, in the elongation phase of spermiogenesis (Figure 7, see steps 9 and 11), and then in coordination with the descent of the manchette at the end of the elongation phase (step 13), is transported to its place of assembly in the postacrosomal region of the sperm head. By step 14, the PAS is fully formed and the manchette has completely detached from the sperm head and begins to deteriorate in the cytoplasmic lobe of the spermatid.

Discussion

Our findings show biochemical and structural evidence for the localization of two distinct isoforms of GSTO2 within the PAS region of the PT in mature mammalian spermatozoa. The larger 31 kDa isoform of GSTO2 has a unique amino terminal extension not previously recorded in the GeneBank, which contains a high percentage of cysteine residues (7%).

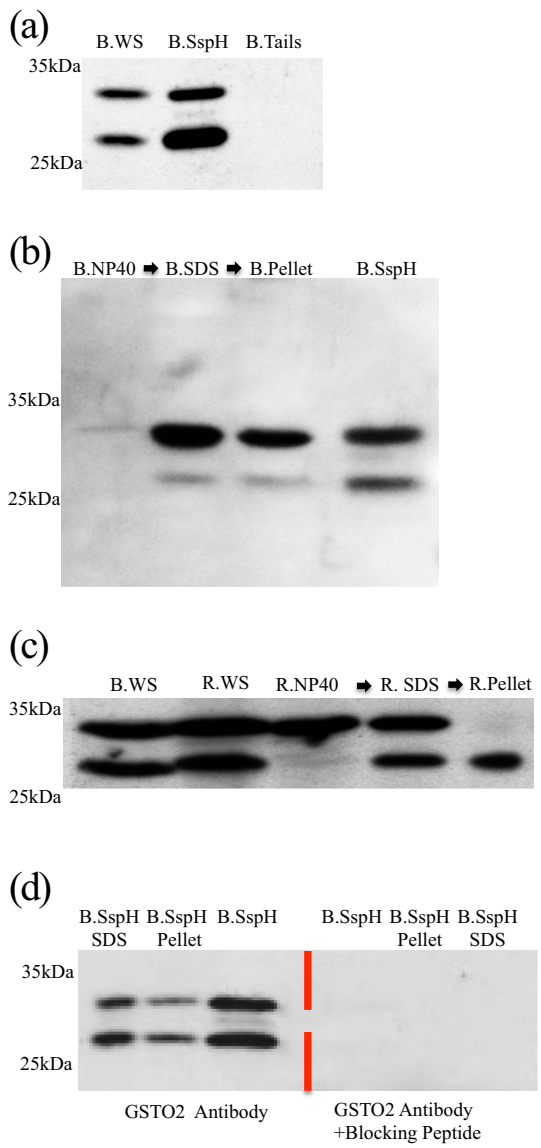

Figure 4. (A) Two immunoreactive bands of 28 and 31 kDa corresponding to the two GSTO2 isoforms are present within bovine whole sperm (B.WS) and in bovine sonicated sperm heads (B.SspH). No GSTO2 labeling is seen within bovine sperm tails (B.Tails; antibody used: Anti-GSTO2, Sigma SAB1401977). (B) The two GSTO2 isoforms within bovine whole sperm are neither extractable with NP40 (B.NP40) nor can they be fully extracted with SDS (B.SDS; antibody used: Anti-GSTO2, Santa Cruz Y-12). GSTO2 is still present in the pellet after the serial detergent extractions (B.Pellet) suggesting some GSTO2 isoforms are covalently bound to the PAS or trapped within this structure. A comparison with sonicated bovine sperm heads (B.SspH) indicates that the two isoforms do reside in the head of bovine spermatozoa. Similar results were also found in mouse and swine (not shown). (Antibody used: Anti-GSTO2, Santa Cruz Y-12). (C) The 28 and 31 kDa immunoreactive bands corresponding to the two GSTO2 isoforms are present within rat spermatozoa (R.WS) at the same levels as seen in bovine whole spermatozoa (B.WS; antibody used: Anti-GSTO2, Santa Cruz Y-12). The upper band is partially extractable with NP40 (R.NP40), and fully extracted with SDS (R.SDS). The lower band shows a higher insolubility and is only partially extractable with SDS, with protein left in the pellet. (Antibody used: Anti-GSTO2, Santa Cruz Y-12). (D) The immunoreactivity of the 28 and 31 kDa bands is fully blocked when the anti-GSTO2 antibody (Santa Cruz Y-12) is preincubated with its sequence-specific blocking peptide (Santa Cruz Y-12P). B.SspH = bovine sonicated sperm heads, B. SspH SDS = the supernant of the SDS extraction of bovine sonicated sperm heads, and B. SspH Pellet = bovine SDS extraction pellet.

GSTO2 is one of only two functional enzymes in the newest class of GST proteins, the Omegas [28]. The GSTs are phase II detoxification enzymes that use reduced glutathione to help conjugate reactions with the electrophilic centers of substrates and act in various detoxification pathways. The GSTs of the Omega (GSTO) class are a unique subset as they have a cysteine at their active site and an unusual N-terminal extension that other GST structures lack [29]. It has been suggested that this structural positioning of the active site and N-terminus may be a key feature in facilitating thiolation in GSTOs [30]. It is theorized that the presence of cysteine at the active site—rather than the serine or tyrosine seen in other GST subfamilies—may also contribute to GSTO's dehydroascorbate reductase activity [31]. The GSTOs also have similar protein folds to glutaredoxins, proteins implicated in antioxidant defenses by reducing dehydroascorbate, peroxiredoxins, and methionine sulfoxide reductases [29]. The structural similarities between GSTOs and the glutaredoxin family of proteins as well as the presence of many of its antioxidant agents within spermatozoa such as dehydroascorbate, perioxiredoxins, and thioredoxins may suggest a similarity in their functions [29, 32, 33].

Fluorescent immunocytochemistry confined the GSTO2 isoforms to the PAS region of the PT in spatulated-shaped sperm heads (i.e, human, bovine and boar), but additionally to the perforatorium of falciform-shaped sperm heads (i.e., rat and mouse). The perforatorial localization of GSTO2 is not surprising as the triangular subacrosomal space, which accommodates the perforatorial proteins, forms during the elongation phase of spermatid head development at the time of PAS assembly [34]. These findings suggest that GSTO2 deposition in the perforatorial region may happen in tandem to its assembly in the PAS region of the PT. In fact, PERF15, the most prominent perforatorial protein begins to associate with the subacrosomal space only after the spermatid elongation phase has begun. Both GSTO2 and PERF15 start to associate with the subacrosomal space at similar times suggesting GSTO2 and PERF15 may utilize the same mechanism of transport to get to their common destination. Interestingly, the perforatorial proteins that occupy the triangular subacrosomal space do not condense to form a definitive electron dense perforatorial structure until the last step of spermiogenesis [34].

The localization and species conservation of GSTO2 within the PAS may suggest that it plays a vital role in the early stages of fertilization. When spermatozoa reach the oocyte during fertilization, fusion of their respective plasma membranes first occurs over the equatorial segment region and then proceeds caudally along the sperm head exposing the PAS to the ooplasm and leading to its immediate solubilization. This immediate access of PAS proteins at the site of fertilization has implicated them in the early stage fertilization processes such as oocyte activation and pronuclear formation [9, 17, 18, 35–36]. Therefore, the possibility exists that GSTO2 is initially involved in the reduction of S–S bonds within the PT during capacitation and/or the early stages of fertilization to allow for its quick dissolution.

Upon sperm–oocyte fusion, the sperm chromatin decondenses, and forms a paternal pronucleus, which then aposes with the haploid genetic complement of the female to form the diploid zygote. It has been shown that oocyte-produced glutathione is essential in the reduction of disulfide bonds in the sperm nucleus during fertilization and the formation of the paternal pronucleus [35, 36]. This disulfide bond reducing agent also appears to be required for the breakdown of the sperm tail connecting piece and in the conversion of the male centriole to an active zygotic microtubule organizing center in most species except the murids [35, 36]. Therefore, the presence of a

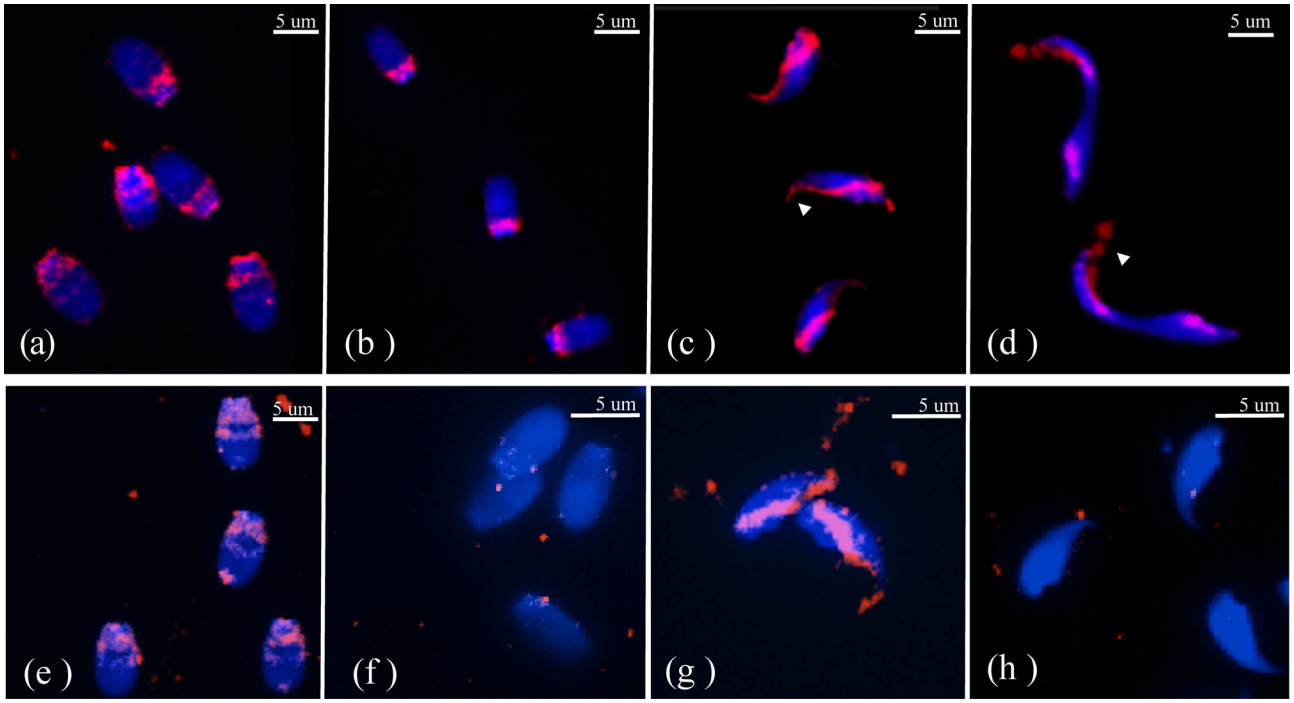

Figure 5. The localization of GSTO2 in mature bovine (A), porcine (B), murine (C), and rat (D) spermatozoa fixed in 4% paraformaldehyde and permeabilized with Triton-X-100 (Anti-GSTO2, Santa Cruz Y-12). Anti-GSTO2(Y-12) labeling in bull (E) and mouse (G) sperm heads fixed in 4% paraformaldehyde and permeabilized with Triton-X-100. Anti-GSTO2 (Santa Cruz Y-12) labeling in bull (F) and mouse (H) sperm heads when the antibody is preincubated with the blocking peptide (Santa Cruz Y-12P). Blue = DAPI, red = GSTO2. [A color version of this figure is available in the online version.]

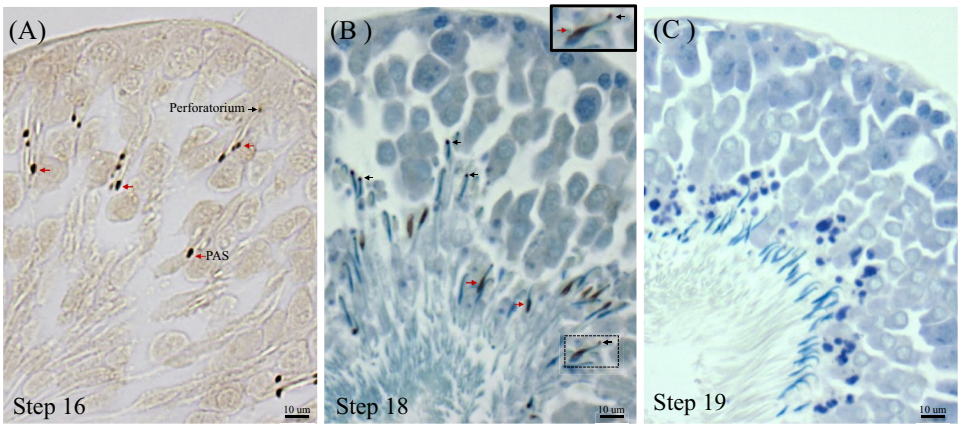

Figure 6. Sections of rat testis fixed in Bouin's, embedded in paraffin and immunostained with anti-GSTO2 antibody (Sigma HPA048181). The GSTO2 immunoreactivity of elongating spermatids is shown as a dark brown stain and indicated by red arrows in the PAS region of the PT and by black arrows in the perforatorium of the PT. (A) Elongated spermatids in step 16 of spermiogenesis soon after the PAS have assembled (red arrows). In these spermatids, the perforatorial region has not yet condensed and thus the immunostaining is not as prominent (black arrows). (B) Elongated spermatids in step 18 of spermiogenesis showing prominent GSTO2 reactivity in both the PAS and perforatorial regions of the PT. (C) Negative control of elongated spermatids in step 19 of spermiogenesis ready for spermiation. Rabbit preimmune serum was used in place of primary antibody. Section A was not counterstained with methylene blue. [A color version of this figure is available in the online version.]

reductive–oxidative enzyme, such as GSTO2, in the vicinity of the decondensing sperm head in the oocyte appears essential to recycle glutathione by continually oxidizing it.

GSTO2, like other known PAS proteins, is transported and deposited into the PAS region during the elongation phase of spermiogenesis [1, 17]. During rat spermiogenesis, GSTO2 is assembled along the caudal region of the elongating sperm heads between steps 15 and 16, when the manchette is finalizing the shaping of the spermatid nucleus and descending down the forming sperm head [16, 17]. The colocalization of GSTO2 and tubulin on the microtubular manchette during spermatid elongation supports the proposed IMT hypothesis. Our findings support the hypothesis that the manchette acts as a transport vessel for specific proteins and aids in their deposition and confinement to specific regions within the elongating head as it develops [11, 16–18].

In summary, the localization of GSTO2 isoforms within the PT, taken together with GSTO's function as an oxidative–reductive enzyme with high thiolation capability, implicates GSTO2 as a

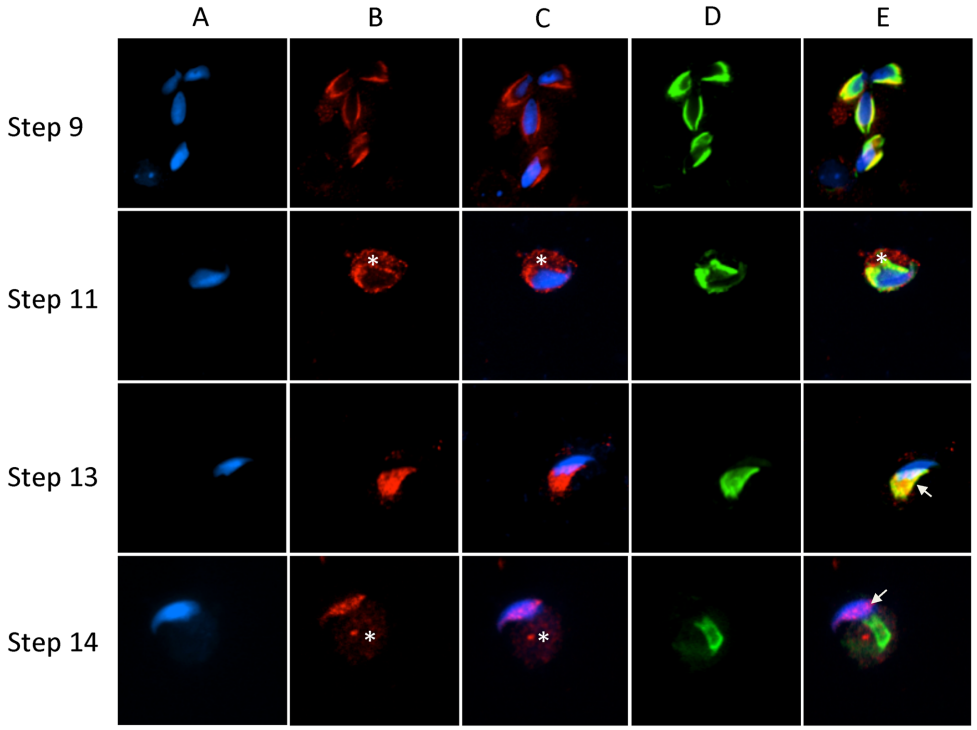

Figure 7. The association of GSTO2 (Anti-GSTO2, Santa Cruz Y-12) and α-tubulin (Sigma, T6074) throughout the 16 steps of mouse spermiogenesis. Mouse spermatids from testicular extracts were fixed in 4% paraformaldehyde and permeabilized after fixation with Triton-X-100. (A) DAPI alone. (B) Anti-GSTO2 antibody alone. (C) Merge A and B. (D) Anti-tubulin antibody alone. (E) A, B, and D merged. Note in steps 13 and 14 that GSTO2 assembles as part of the PAS (arrows). Blue = DAPI, red = anti-GSTO2 (Y-12), green = anti-tubulin, yellow = the colocalization of GSTO2 and tubulin, asterisk = cytoplasmic lobe, and bar = 5 μm. [A color version of this figure is available in the online version.]

potential candidate in the dissolution of sperm structures surrounding and within the nucleus, a preliminary requirement for the formation of the male pronucleus during the initial phases of fertilization.

Acknowledgments

We would like to express our appreciation to Matt Gordon and Jeff Mewburn of the Queen's University Biomedical Imaging Centre for their guidance and assistance in image acquisition and analysis.

References

1. Oko R, Sutovsky P. Biogenesis of sperm perinuclear theca and its role in sperm functional competence and fertilization. *J Reprod Immunol* 2009; **83**:2–7.
2. Courtens JL, Courot M, Flechon JE. The perinuclear substance of boar, bull, ram and rabbit spermatozoa. *J Ultrastruct Res* 1976; **57**:54–64.
3. Lalli M, Clermont Y. Structural changes of the head components of the rat spermatid during late spermiogenesis. *Am J Anat*1981; **160**:419–434.
4. Olson GE, Noland TD, Winfrey VP, Garbers DL. Substructure of the postacrosomal sheath of bovine spermatozoa. *J Ultrastruct Res* 1983; **85**:204–218.
5. Longo FJ. Basic proteins of the perinuclear theca of mammalian spermatozoa and spermatids: a novel class of cytoskeletal elements. *J Cell Biol* 1987; **105**:1105–1120.
6. Olson GE, Winfrey VP. Characterization of the postacrosomal sheath of bovine spermatozoa. *Gamete Res* 1988; **20**:329–342.
7. Oko R, Maravei D. Protein composition of the perinuclear theca of bull spermatozoa. *Biol Reprod* 1994; **50**:1000–1014.
8. Barth AD, Oko R. *Abnormal Morphology of Bovine Spermatozoa*. Ames: Iowa State University Press; 1989;
9. Oko R, Maravei D. Distribution and possible role of perinuclear theca proteins during bovine spermiogenesis. *Microsc Res Tech* 1995; **32**:520–532.
10. Clermont Y, Oko R, Hermo L. Cell and molecular biology of the testis. *Cell Biology of Mammalian Spermatogenesis*. New York: Oxford University Press; 1993:332–376.
11. Russell LD, Russell JA, Macgregor GR, Meistrich ML. Linkage of manchette microtubules to the nuclear envelope and observations of the role of the manchette in nuclear shaping during spermiogenesis in rodents. *Am J Anat* 1991; **192**:97–120.
12. Meistrich ML, Trostle-Weige PK, Russell LD. Abnormal manchette development in spermatids ofazh/azh mutant mice. *Am J Anat* 1990; **188**:74–86.
13. Kierszenbaum AL. Spermatid manchette: plugging proteins to zero into the sperm tail. *Mol Reprod Dev* 2001; **59**:347–349.
14. Hall ES, Eveleth J, Jiang C, Redenbach DM, Boekelheide K. Distribution of the microtubule-dependent motors cytoplasmic dynein and kinesin in rat testis. *Biol Reprod* 1992; **46**:817–828.
15. Miller MG, Mulholland DJ, Vogl AW. Rat testis motor proteins associated with spermatid translocation (dynein) and spermatid flagella (kinesin-II). *Biol Reprod* 1999; **60**:1047–1056.
16. Kierszenbaum AL. Intramanchette transport (IMT): managing the making of the spermatid head, centrosome, and tail. *Mol Reprod Dev* 2002; **63**:1–4.
17. Tovich PR, Sutovsky P, Oko RJ. Novel aspect of perinuclear theca assembly revealed by immunolocalization of non-nuclear somatic histones during bovine spermiogenesis. *Biol Reprod* 2004; **71**:1182–1194.
18. Wu ATH, Sutovsky P, Xu W, Van Der Spoel AC, Platt FM, Oko R. The postacrosomal assembly of sperm head protein, PAWP, is independent of acrosome formation and dependent on microtubular manchette transport. *Dev Biol* 2007; **312**:471–483.

19. Aul RB, Oko RJ. The major subacrosomal occupant of bull spermatozoa is a novel histone H2B variant associated with the forming acrosome during spermiogenesis. *Dev Biol* 2002; **242**:376–387.
20. Mountjoy JR, Xu W, Mcleod D, Hyndman D, Oko R. RAB2A: a major subacrosomal protein of bovine spermatozoa implicated in acrosomal biogenesis. *Biol Reprod* 2008; **79**:223–232.
21. Tran MH, Aul RB, Xu W, Van Der Hoorn FA, Oko R. Involvement of classical bipartite/karyopherin nuclear import pathway components in acrosomal trafficking and assembly during bovine and murid spermiogenesis. *Biol Reprod* 2012; **86**:84–94.
22. Tovich PR, Oko RJ. Somatic histones are components of the perinuclear theca in bovine spermatozoa. *J Biol Chem* 2003; **34**:32431–32438.
23. Wu ATH, Sutovsky P, Manandhar G, Xu W, Katayama M, Day BN, Park K, Yi Y, Xi YW, Prather RS, Oko R. PAWP, a sperm-specific WW domain-binding protein, promotes meiotic resumption and pronuclear development during fertilization. *J Biol Chem* 2007; **282**:12164–12175.
24. Aarabi M, Balakier H, Bashar S, Moskovtsev SI, Sutovsky P, Librach CL, Oko R. Sperm-derived WW domain-binding protein, PAWP, elicits calcium oscillations and oocyte activation in humans and mice. *FASEB J* 2014; **28**:4434–4440.
25. Laemmli UK. Cleavage of structural proteins during the assembly of the head of bacteriophage T4. *Nature* 1970; **227**:680–685.
26. Towbin H, Staehelin T, Gordon J. Electrophoretic transfer of proteins from polyacrylamide gels to nitrocellulose sheets: procedure and some applications. *Proc Natl Acad Sci U S A* 1979; **76**:4350–4354.
27. Oko RJ, Jando V, Wagner CL, Kistler WS, Hermo LS. Chromatin reorganization in rat spermatids during the disappearance of testis-specific histone, H1t, and the appearance of transition proteins TP1 and TP21. *Biol Reprod* 1996; **54**:1141–1157.
28. Whitbread AK, Masoumi A, Tetlow N, Schmuck E, Coggan M, Board PG. Characterization of the omega class of glutathione transferases. *Meth Enzymol* 2005; **401**:78–99.
29. Board PG. The omega-class glutathione transferases: structure, function, and genetics. *Drug Metab Rev* 2011; **43**:226–235.
30. Nebert DW, Vasiliou V. Analysis of the glutathione S-transferase (GST) gene family. *Hum Genomics* 2004; **1**:460–464.
31. Hemachand T, Gopalakrishnan B, Salunke DM, Totey SM, Shaha C. Sperm plasma-membrane-associated glutathione S-transferases as gamete recognition molecules. *J Cell Sci* 2002; **115**:2053–2065.
32. Miranda-Vizuete A, Sadek CM, Jiménez A, Krause WJ, Sutovsky P, Oko R. The mammalian testis-specific thioredoxin system. *Antioxid Redox Signal* 2004; **6**:25–40.
33. O'flaherty C. Peroxiredoxins: hidden players in the antioxidant defence of human spermatozoa. *Basic Clin Androl* 2014; **24**:4–13.
34. Oko R, Clermont Y. Origin and distribution of perforatorial proteins during spermatogenesis of the rat: an immunocytochemical study. *Anat Rec* 1991; **230**:489–501.
35. Sutovsky P, Manandhar G, Wu A, Oko R. Interactions of sperm perinuclear theca with the oocyte: Implications for oocyte activation, antipolyspermy defense, and assisted reproduction. *Microsc Res Tech* 2003; **61**:362–378.
36. Sutovsky P, Schatten G. Depletion of glutathione during bovine oocyte maturation reversibly blocks the decondensation of the male pronucleus and pronuclear apposition during fertilization. *Biol Reprod* 1997; **56**:1503–1512.